Superferromagnetism in chain-like Fe@SiO2 nanoparticle ensembles

A. Zeleáková, V. Zeleák, I. Mat'ko, M. Streková, P. Hrubovák, and J. Ková

Citation: Journal of Applied Physics **116**, 033907 (2014); doi: 10.1063/1.4890354
View online: http://dx.doi.org/10.1063/1.4890354
View Table of Contents: http://scitation.aip.org/content/aip/journal/jap/116/3?ver=pdfcov
Published by the AIP Publishing

Superferromagnetism in chain-like Fe@SiO_2 nanoparticle ensembles

A. Zeleňáková,[1,a)] V. Zeleňák,[2] I. Mat'ko,[3] M. Strečková,[4] P. Hrubovčák,[1] and J. Kováč[5]
[1]*Department of Condensed Mater Physics, P. J. Šafárik University, Park Angelinum 9, Košice, Slovakia*
[2]*Department of Inorganic Chemistry, P.J. Šafárik University, Moyzesova 11, Košice, Slovakia*
[3]*Institute of Physics, Slovak Academy of Sciences, Dúbravská cesta 9, 845 11 Bratislava, Slovakia*
[4]*Institute of Material Science, Slovak Academy of Sciences, Watsonova 41, Košice, Slovakia*
[5]*Institute of Experimental Physics, Slovak Academy of Sciences, Watsonova 41, Košice, Slovakia*

(Received 2 April 2014; accepted 4 July 2014; published online 16 July 2014)

One-dimensional (1D) chain-like nanocomposites, created by ensembles of nanoparticles of with diameter ~ 13 nm, which are composed of an iron core (~4 nm) and a silica protective layer, were prepared by a self-assembly process. Chain-like Fe@SiO_2 ensembles were formed due to strong magnetic dipole–dipole interactions between individual Fe nanoparticles and the subsequent fixation of the Fe particles by the SiO_2 layers. X-ray near edge absorption spectra measurements at the Fe K absorption edge confirm that the presence of a silica layer prevents the oxidation of the magnetic Fe core. Strong magnetic interactions between Fe cores lead to long-range ordering of magnetic moments, and the nanoparticle ensembles exhibit superferromagnetic characteristics demonstrated by a broad blocking Zero-field cooling (ZFC)/field-cooling distribution, nearly constant temperature dependence of ZFC magnetization, and non-zero coercivity at room temperature. Low room-temperature coercivity and the presence of electrically insulating SiO_2 shells surrounding the Fe core make the studied samples suitable candidates for microelectronic applications.
 [http://dx.doi.org/10.1063/1.4890354]

I. INTRODUCTION

Mono-domain metal nanoparticles (NPs) based on iron or cobalt are of great interest due to their intrinsic physical properties, such as macroscopic quantum tunneling (MQT), quantum size effects, giant magnetic moment, and the interplay between core atoms and frustrated surface spins.[1–4] In particular, metal nanoparticles have attracted the attention of the scientific community because of their applications in information storage technologies or in biomedicine as contrast agents for magnetic resonance imaging, carriers in drug or gene delivery systems, or materials for hyperthermal treatment of tumors.[5–7]

However, the above mentioned physical properties can be significantly affected by competing interactions between nanoparticles.[4–8] Therefore, a deep understanding of interparticle interactions is crucial for their subsequent practical applications. Weak interparticle magnetic interactions lead to the superparamagnetic (SPM) behavior. In contrast, strongly interacting and dense NPs systems show spin glass (SG) behavior, and in analogy with atomic spin glasses are referred to as superspin glasses (SSG).[9–11] At higher NP densities and even stronger interactions between superspins, a so-called superferromagnetic (SFM) state is formed in which the superspins of all NPs are correlated in a ferromagnetic-like fashion.[12,13]

SFM was first observed and described by Morup *et al.*[14] in 10–100 nm goethite nanoparticles. It was found that the magnetic properties of the microcrystalline goethite could not be described by existing theories for collective magnetic excitations and superparamagnetic relaxation. However, a modification of Weiss's mean field theory for interacting particles gave an excellent fit to their results, and this model was denoted "super-ferromagnetism." A SFM character has subsequently been observed in discontinuous metal-insulator multilayers in which magnetic percolation is mediated by ultrasmall paramagnetic particles between the superspins.[15,16] Bedanta *et al.*[16,17] reported the suppression of dipolar disorder among the superspins in dense CoFe nanoparticle ensembles leading to the long-range ordered SFM state. Similarly, Alonso *et al.*[18] observed the crossover from SSG to SFM behavior in FeAg thin films. At lower concentrations of Fe nanoparticles, a collective freezing of the magnetic moments was observed; whereas at higher concentrations, direct exchange interactions were present between Fe nanoparticles. Jiménez-Villacorta *et al.*[19] reported evidence of modification of the magnetic behavior of NPs evoked by the interaction effects between Fe clusters in granular Fe/Si_3N_4 particles. The sample with very small Fe cluster dimensions showed superparamagnetic features due to weak dipolar interactions; while in the sample with larger Fe clusters, stronger interactions led to superferromagnetism.[19]

The SFM state, characterized by ferromagnetic interparticle correlations, was associated by many authors with high concentration of the nanoparticles and/or with an increase of their size.[12–19] However, the growth of NPs can also cause a shift from mono-domain particles to multi-domain ferromagnets, thereby invalidating the simplifying superspin approximation. Therefore, it is of strong interest to modify the magnetic properties of nanoparticles while preserving the mono-domain state. One approach to shifting the behavior of a nanoparticle ensemble from superparamagnetic to superferromagnetic is the creation of chain-like structures.

Chain-like Fe nanoparticles coated by a silica (SiO_2) layer were studied by Yang *et al.*[20] Fe@SiO_2 nanoparticle polymer composites were prepared with uniform size

a)Email: adriana.zelenakova@upjs.sk

distribution of NPs, which exhibited improved magneto-dielectric properties (dielectric permittivity (ε), magnetic permeability (μ) and dielectric loss ($\tan\delta$)) at radio frequencies (1 MHz–1 GHz). This phenomenon of chain-like nanoparticles has also been reported for cobalt and nickel systems.[21,22] Salgueirino-Maceira *et al.*[21] reported strong magnetic interactions due to the self-assembly of silica-coated cobalt nanoparticles organized into one-dimensional chains creating unique pearl necklaces. The transition from the superparamagnetic to superferromagnetic (SPM–SFM) state was observed as a function of increasing nanoparticle size.

In our work, we describe the preparation of Fe nanoparticles coated with a SiO_2 layer using surface-capping agents (oleic acid and citric acid). The silica layer prevents oxidation of the surface of the iron cores and promotes the self-assembly of nanoparticles into chain-like structures. The samples were studied by powder X-ray diffraction (XRD), high resolution transmission electron microscopy (HRTEM), X-ray absorption near edge spectra (XANES), and magnetic measurements including the temperature and field dependence of the magnetization.

II. EXPERIMENTAL PROCEDURE

A. Materials

All chemicals, namely iron nitrate ($Fe(NO_3)_3.9H_2O$), oleic acid (OA), citric acid (CA), tetraethyl orthosilicate (TEOS), 3-(aminopropyl)trimethoxysilane (APS), and sodium borohydride ($NaBH_4$; 98%) were purchased from Aldrich and used as received without further purification.

B. Synthesis of pristine iron nanoparticles

Citric acid (CA) and oleic acid (OA) were used as surfactants and stabilizing agents of iron nanoparticles. In a typical synthesis. iron (III) nitrate, citric acid (CA), and oleic acid (OA) in a molar ratio (Fe^{3+}/CA/OA) = 1/1/0.5 were dissolved in a 200 cm^3 water/ethanol (2:1, v/v) mixture. Then, 20 cm^3 of 0.15 M solution of $NaBH_4$ was dropped into the reaction mixture. The final mixture was stirred for 20 min and the precipitated nanoparticles were separated by centrifugation at 4000 rpm.

C. Synthesis of silica coated Fe nanoparticles (Fe@SiO_2)

Fe@SiO_2 nanoparticles were prepared by the procedure described above, but in the final stage of the synthesis, before the separation of the nanoparticles, 40 μl of APS and 200 μl of TEOS were added into the suspension to coat the Fe nanoparticles with SiO_2 layers.[23] The suspension was stirred for 30 min. The Fe@SiO_2 nanoparticles were separated by centrifugation at 4000 rpm, washed with ethanol and vacuum dried.

D. Characterization

The structural characterization of the prepared pristine Fe nanoparticles and Fe@SiO_2 nanocomposite was performed using HRTEM and synchrotron radiation related techniques.

The HRTEM micrographs were taken with a JEOL 2100F microscope. A copper grid coated with a holey carbon support film was used to prepare samples for the TEM observation. The bright-field TEM image was obtained at 200 kV. The particle size reported as average observed size (D_{avg}) was measured as average particle size from multiple TEM images.

The high-energy powder X-ray diffraction (HE-PXRD) experiments were carried out at the BW5 wiggler beamline of the DORIS positron storage ring in DESY (Hamburg, Germany) using monochromatic synchrotron radiation with beam energy of 100 keV ($\lambda = 0.12398$ Å). The samples were measured at room temperature in the transmission mode. LaB_6 standard was used to calibrate the sample-to-detector distance. The background intensity was subtracted directly from XRD patterns, and the result was integrated to the Q-space ($Q = 4\pi \sin(\theta)/\lambda$) using the software package FIT2D.[24]

The XANES measurements were done at B1 Hasylab beamline (DESY Hamburg). The sample powder was spread on and sealed between two pieces of kapton tape. The transmission of the sample was determined by measuring the X-ray intensity with an ionization chamber in front of the sample and a photodiode behind it. The energy scale was calibrated using the 1st inflection points of Fe, Ni, and Se foils.[25]

The magnetic measurements were performed on a commercial SQUID-based magnetometer (Quantum Design MPMS 5XL) over a wide range of temperatures (2–300 K) and applied dc fields (up to 5 T). Zero-field cooling (ZFC) and field-cooling (FC) temperature-dependent magnetization $M(T)$ measurements were carried out in dc mode. The samples were encapsulated in a plastic sample holder. The diamagnetic contribution of plastic capsule and plastic sample holder is insignificant in comparison with high magnetic moment of the sample and no correction was necessary.

III. RESULTS AND DISCUSSION

To demonstrate the influence of the SiO_2 coating layer on the properties of the Fe nanoparticles, two comparable samples, pristine nanostructured Fe and silica coated Fe (Fe@SiO_2) were studied.

A. Structural properties

Figs. 1(a) and 1(b) show bright field TEM images of pristine Fe nanoparticles. It can be seen that the pristine Fe nanoparticles are densely packed and create randomly oriented ensembles. Selected area electron diffraction (SAED) patterns (Fig. 1(c)) showed the partially crystalline character of the sample. The powder aggregates are composed of nearly spherical nanoparticles with an average size of $D_{avg} = 3.8 \pm 0.1$ nm, as estimated from the particle size distribution (Fig. 1(d)).

The TEM micrographs of the Fe@SiO_2 sample are shown in Figs. 2(a) and 2(b). For the better eye guidance, Fe core and SiO_2 coating layer were marked with circles in Fig. 2(a). It can be seen from the images that the Fe@SiO_2 particles are arranged in 1D chains, in contrast to the randomly organized ensembles in pristine Fe NPs.

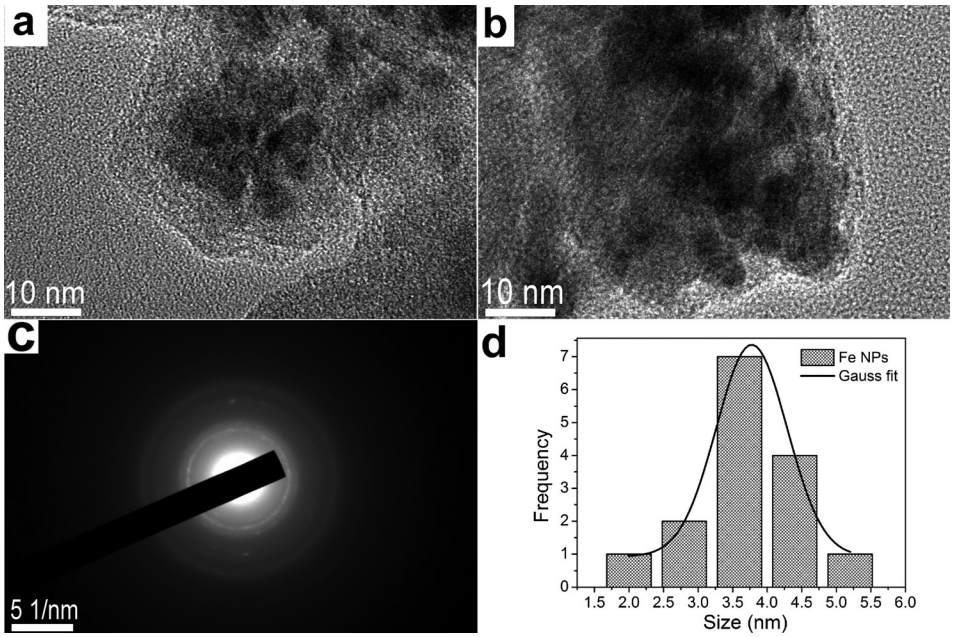

FIG. 1. High resolution transmission electron images of pristine Fe nanoparticle sample. (a), (b) Bright field TEM images. (c) SAED pattern. (d) Normalized histogram of particle size distribution.

These TEM results suggest that the silica layer promotes the creation of chain-like structures. This observation was also reported by other authors for various metallic systems.[20–22] In the SAED pattern measured on the silica coated sample (Fig. 2(c)), no distinct diffraction spots were present, which is a consequence of the amorphous silica shell deposited on the surface of the Fe nanoparticles. A similar observation was reported by Kobayashi *et al.*[22] for monodispersed Co nanoparticles coated with a silica layer.

The average Fe@SiO_2 particle size, as estimated from bright field TEM images, was $D_{avg} = 13.4 \pm 0.4$ nm (Fig. 2(d)). The approximate size of the Fe nanoparticles embedded inside the silica protective layer was similar to the pristine Fe sample (approximately 4 nm).

In both nanoparticle samples (Fe and Fe@SiO_2), the nanoparticles are covered by the residuals of the surfactant, used in the synthesis. The "cloud" observed around the nanoparticles (see Fig. 2(a)) is formed by organic surfactant molecules. The presence of such organic layer has no influence on the magnetic properties and this layer itself cannot protect the Fe nanoparticles from the oxidation, as it was documented for pristine Fe nanoparticles (see below).

The XRD patterns of the pristine Fe nanoparticles and the Fe@SiO_2 sample are shown in Fig. 3. The Bragg peaks present in the patterns have large full width at half maximum indicating the nanostructured character of the particles. The peaks in the Fe@SiO_2 sample are less pronounced in comparison with the pristine Fe NPs due to the presence of the amorphous silica layer on their surface.

The XRD patterns of both samples show the presence of *bcc* iron nanoparticles (JCPDS-ICDD No. 60696), with diffraction peaks at 2θ values of 3.505, 4.958, 6.073, 7.014,

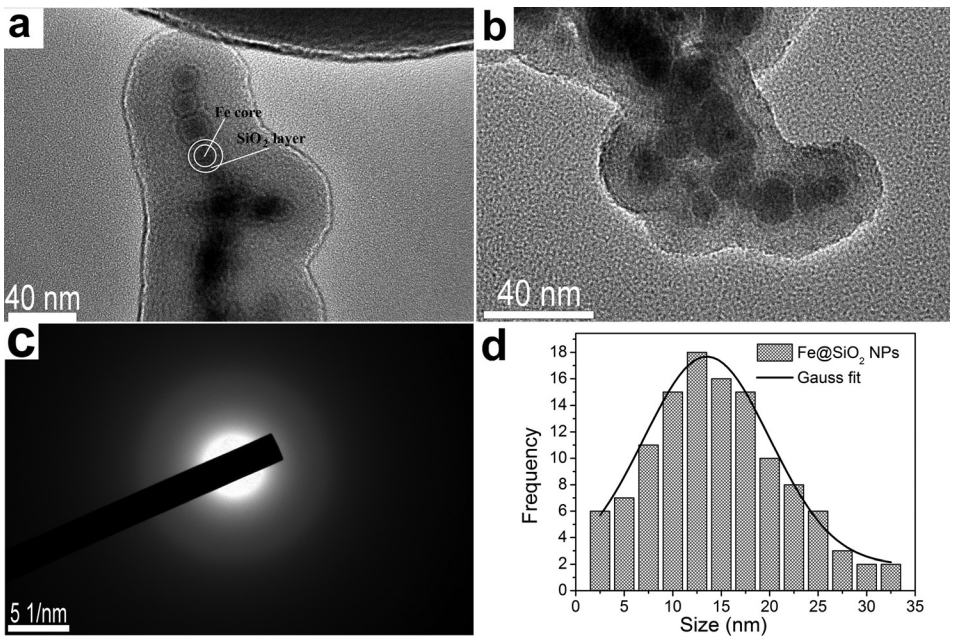

FIG. 2. High resolution transmission electron images of Fe@SiO_2 nanoparticles sample. (a), (b) Bright field TEM images. (c) SAED pattern. (d) Normalized histogram of particle size distribution. For the better eye guidance Fe core and SiO_2 coating layer were marked with circles in part (a) of the figure.

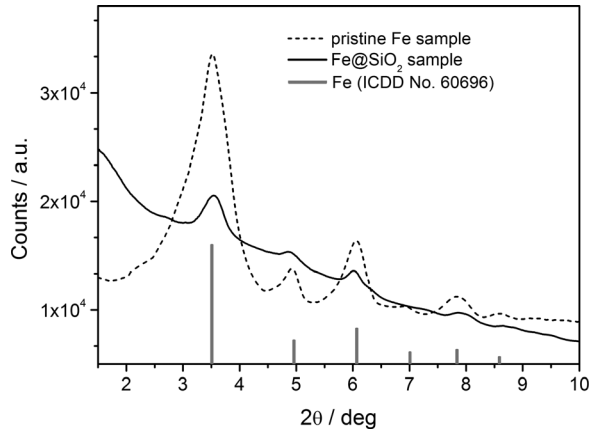

FIG. 3. Room-temperature HE-XRD patterns of pristine Fe nanoparticles (dashed line) and coated $Fe@SiO_2$ NPs (solid line).

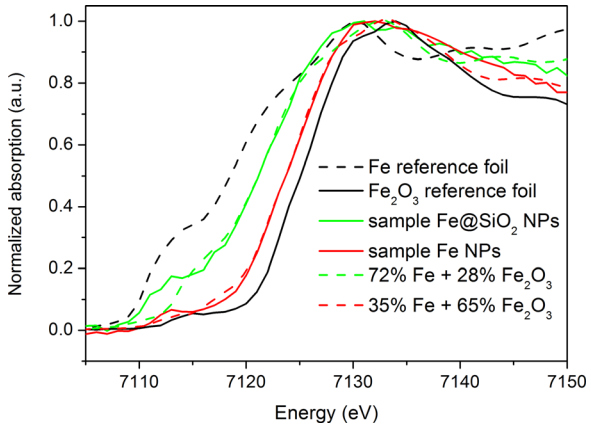

FIG. 4. Experimental XANES spectra at Fe *K edge* measured on the Fe reference foil (black dashed line), Fe_2O_3 reference foil (black solid line) and studied nanoparticles samples of Fe NPs (red line) and $Fe@SiO_2$ NPs (green line) at same conditions. Dashed green and red lines were obtained by fitting of the XANES spectra with a combination of the reference Fe and Fe_2O_3 foils.

7.843, and 8.592°, corresponding to (1 1 0), (2 0 0), (2 1 1), (2 2 0), (3 1 0), and (2 2 2) reflections, respectively. According the HE-XRD results, only the *bcc* iron phase was present in both samples. However, Yang *et al.*[20] reported that the Fe core of $Fe@SiO_2$ nanoparticles can gradually oxidize to form a thin layer of FeO. Also, Sun *et al.*[26] investigated the structural properties of zero-valent Fe nanoparticles and observed that 60 nm iron particles exhibited a tendency towards surface oxidation. They reported that the nominally iron nanoparticles were composed of a core of zero-valent iron and a shell of iron oxides.[26] The oxidation products in the XRD data of our samples were not observed supposedly due to the low concentration of oxidized species (under the detection limit of the XRD method) as well as large full widths at half maximum (FWHM) of the diffraction peaks. However, as it follows from the other methods or above cited references, partial surface oxidation of metals usually takes place.

To investigate the possible surface oxidation of prepared iron nanoparticles we have performed XANES measurements for both samples. Such measurements, which provide information about electron configuration are sensitive to the oxidation state of the absorbing atom. As it is seen from Fig. 4, the XANES spectrum at the Fe K edge of the $Fe@SiO_2$ sample closely resembles that of the Fe reference foil, which has a significant shoulder around 7113 eV. However, a small upshift of the XANES spectrum of the $Fe@SiO_2$ sample (green line) with respect to the Fe reference (black dashed line) was observed. This may indicate that some of the iron atoms have different electron density and a higher oxidation state, although this effect could also be associated with the nano-sized character of the $Fe@SiO_2$ sample in comparison with bulk reference foil. An influence of particle size on the XANES spectra was observed by Cheng *et al.*,[27] who demonstrated that the reactivity of metal nanoparticles towards their environment is inversely proportional to their size. However, we suppose that change and shift of the XANES data is due to partial surface oxidation of the sample. At the "interface" of Fe core and SiO_2 layer, the thin Fe_2O_3 boundary, connecting Fe and SiO_2 phases, may exist. This can explain the observed differences in XANES spectra. In any case, the oxide layer was formed probably only during the sample preparation and bonding of the SiO_2 layer onto Fe nanoparticles and further oxidation, after synthesis and occluding of Fe nanoparticles by silica, do not proceed. It was documented also by magnetic measurements, when the magnetic behavior of the as-synthesized $Fe@SiO_2$ sample and sample measured after three months was the same.

The XANES spectrum of the pristine Fe nanoparticle sample (red solid line in Fig. 4) shows only a small shoulder at 7113 eV in the pre-absorption region and the spectrum is shifted to higher energies closer to the spectrum of the Fe_2O_3 reference foil (black solid line). Moreover, the change in magnetic properties of pristine Fe nanoparticle sample was observed after experiments repeated in three months. The observed behavior of both samples indicates that silica coating in the $Fe@SiO_2$ sample helps to prevent oxidation of Fe NPs. For comparison, Sun *et al.*[26] reported that in uncoated 60 nm particles, the ratio of oxidized surface atoms to zero-valent Fe atoms in the core is about 56%:44%. In our experiments, we have fitted the XANES spectra of Fe and $Fe@SiO_2$ samples with a linear combination of the reference Fe and Fe_2O_3 foils. The obtained results gave Fe: Fe_2O_3 ratios 35%:65% and 72%:28% for the samples Fe and $Fe@SiO_2$, respectively. High content of iron (III) oxide in pristine Fe sample seems to do not agree with the XRD results; however, we have to keep in mind the mentioned gradual oxidation of the sample and the fact that the XANES spectra were measured on the same sample as XRD, but with few weeks delay (beam-time allowance).

B. Magnetic properties of pristine Fe nanoparticles and $Fe@SiO_2$ nanocomposites

The magnetic properties of pristine Fe and $Fe@SiO_2$ samples were investigated using temperature dependence of magnetization (M vs. T) under ZFC/FC protocols in the temperature region of 2–390 K at various external field of 100, 500, 1000, and 5000 Oe and using field dependence of magnetization (M vs. H) in external dc magnetic fields of up to

50 000 Oe. In the Fe NPs sample (Fig. 5(a)), the ZFC and FC curves in dc fields of 500 Oe and 1000 Oe exhibit features typical for nanoparticle systems: (i) the dependence of ZFC magnetization on the temperature reaches a field-dependent maximum, which corresponds to the overcoming of energy barriers due to thermal effects and (ii) high irreversibility between ZFC and FC curves is present below a characteristic temperature. The irreversibility temperature T_{irr} (the temperature above which the ZFC a FC curves merge together) is dependent on the external field, with an average value of $T_{irr} \sim 330$ K–360 K. In an external dc field of 5000 Oe, the ZFC and FC curves are identical.

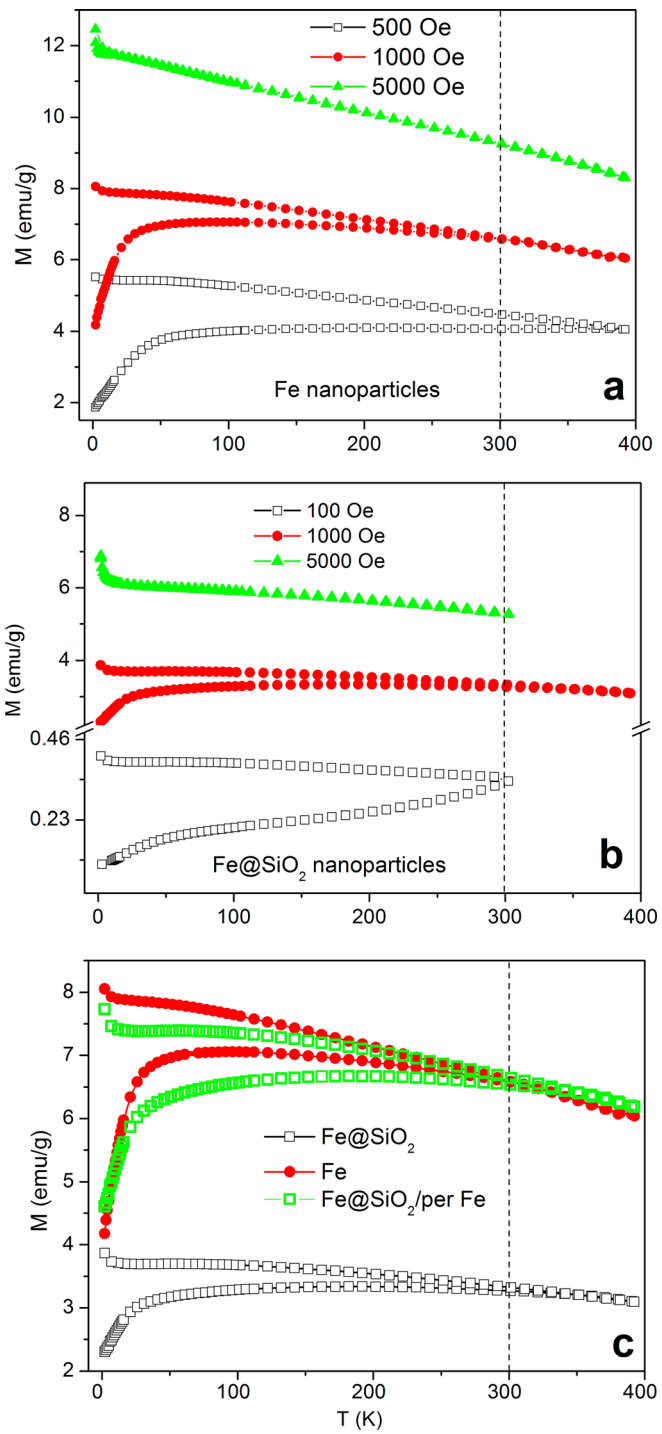

FIG. 5. Temperature dependence of magnetization measured under ZFC and FC protocols and different external dc magnetic fields for (a) pristine Fe nanoparticles and (b) coated $Fe@SiO_2$ nanoparticles. (c) Comparison of ZFC/FC magnetization in an external field of 1000 Oe for Fe (red circles) and $Fe@SiO_2$ (white squares) nanoparticle samples and rescaled magnetization in the $Fe@SiO_2$ sample based on the Fe content (green squares). The dashed line indicates room temperature.

In the $Fe@SiO_2$ sample (Fig. 5(b)), the FC curves at 100 Oe and 1000 Oe show almost constant increase of magnetization with increasing temperature before reaching the FC magnetization values. In the field of 5000 Oe, the ZFC/FC curves merged together over the entire temperature interval. These properties in thermomagnetic ZFC/FC curves are associated with a ferromagnetic behavior.[15–19,28] A similarly shaped ZFC curve, as a result of strong ferromagnetic correlations between particles, has also been observed by Sousa *et al.*[28] in granular $CoFe/Al_2O_3$ multilayers and by Jimenez-Villacorta *et al.*[19] in Fe/Si_3N_4 multilayers. Hansen *et al.*[29] observed that at high particle densities, when the shells are in strong direct contact, the effective thickness of a shell is doubled and the direct exchange coupling interactions between atoms from neighboring particles start to play a role in the system along with classical dipolar interactions.

In addition, the upward turn of FC magnetization was observed in the temperature region 2–9 K in both measured samples. We suggest that such experimental fact demonstrates the transition from SFM to the pure ferromagnetic (FM) state in the low temperature region. The transition from SFM to FM state was observed by Mazaleyrat *et al.*[30] in 1996 at the cooling process of nanocrystalline alloy. The authors note that this transition shows that the magnetic coupling between Fe based grains and the amorphous matrix plays a role in magnetic properties of nanocrystalline systems. Crossover from non-percolated superferromagnetic state to percolated ferromagnetic state was observed also by Bedanta *et al.*[17] in granular thin films consisting from ferromagnetic single-domain particles.

To better understand the influence of the SiO_2 coating layer on the magnetic properties of the nanoparticles, we compared the thermomagnetic curves at the same dc external field. The curves are shown in Fig. 5(c) and they are off-set for better comparison. A significant decrease of magnetization in the $Fe@SiO_2$ sample (white squares) was observed. This was due to the decrease of Fe content in the nanocomposite; therefore, we have rescaled the magnetization value based on the amount of Fe present in the composite. From the comparison of the ZFC/FC curves of Fe (red circles in Figure 5(c)) and $Fe@SiO_2$ (green squares in Fig. 5(c)), it is evident that for the same amount of Fe, the thermomagnetic curves differ. In the $Fe@SiO_2$ sample, the ZFC curves show an almost constant increase in magnetization with increasing temperature before merging with the FC curves. Also, the temperature of ZFC/FC irreversibility T_{irr} is slightly shifted. However, both samples exhibit very strong magnetic interactions demonstrated by a broad blocking distribution, which predicts the appearance of superferromagnetic long-range ordering. As seen from Fig. 5, the ZFC/FC irreversibility region was shifted towards room temperature.

This behavior is in contrast to typical superparamagnetic nanoparticles, which exhibit ZFC/FC irreversibility from

very low temperatures.[31,32] To demonstrate the differences between the samples, we have measured the field dependence of magnetization at 2 K, 300 K, and 390 K (Figs. 6(a)–6(c)).

From Fig. 6(a), it can be clearly seen that the hysteresis loops obtained at 2 K for the pristine Fe sample and the Fe@SiO_2 sample differ. The pristine Fe NPs sample (red squares) exhibits an irregular "wasp-waisted" loop[35] showing the coexistence of two magnetic regimes: magnetically harder and softer, with higher and lower value of magnetic anisotropy constant, respectively. This behavior of the Fe sample, where the magnetization processes are affected by two magnetic regimes was observed at all temperatures, see Fig. 6. In contrast, in the Fe@SiO_2 sample a wider, single phase hysteresis loop (green line) with high magnetic anisotropy was observed. The high value of magnetic anisotropy and higher coercivity ($H_C = 670$ Oe at 2 K) in the Fe@SiO_2 sample could be attributed to the ordering of nanoparticles in 1D chain-like ensembles. In contrast, in the Fe sample, the decrease of coercivity ($H_C = 430$ Oe at 2 K) shows the random magnetic anisotropy from 3D ensembles. We assume that the decreasing coercivity caused by the random anisotropy exhibits the similarity with decreasing coercivity in soft nanocrystalline ferromagnets, which was described by Herzer's random anisotropy model.[33,34] In nanocrystalline ferromagnets, the reducing the grain size below exchange correlation length leads to the decreasing the anisotropy and coercivity.[33]

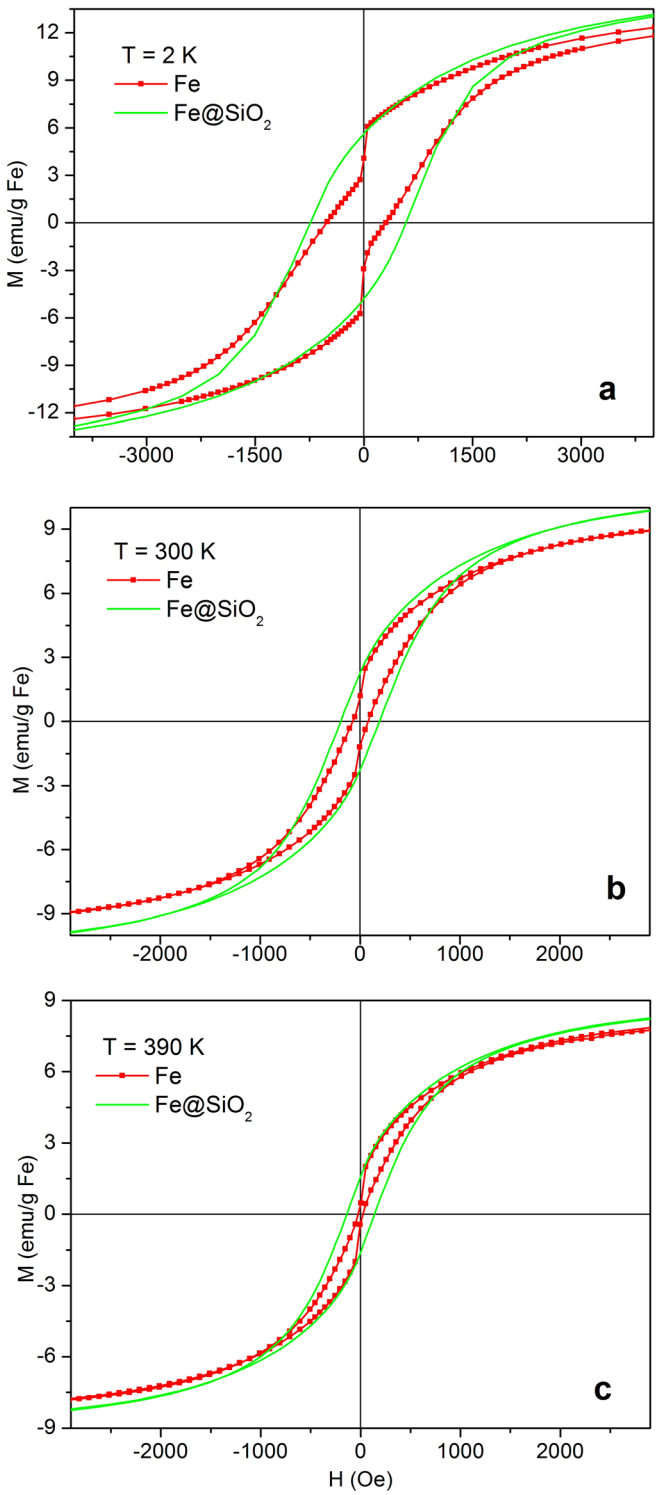

FIG. 6. Field dependence of magnetization for pristine Fe sample and Fe@SiO_2 sample measured at various temperatures (a) 2 K, (b) 300 K, (c) 390 K.

The peculiar hysteresis curve often denoted as a "constricted loop" was observed also by Solzi *et al.* [35] and Lee *et al.* [36] on FePt nanocrystals. Authors[35,36] explained this phenomenon by (i) effect of the surface anisotropy superimposed to bulk anisotropy, (ii) the occurrence of a bimodal NPs size distribution with large multi-domain particles, or (iii) the influence of dipolar interactions, which could affect the hysteresis behavior. Similar mechanisms could be responsible for the irregular hysteresis loop in our studied Fe NPs system.

With increasing temperature, the hysteresis loops become narrower and coercivity decreases. The expected decrease of coercivity to zero (typical in mono-domain nanoparticles due to the SPM character[31,32] was observed neither at 300 K nor at 390 K. Instead, the interactions between particles tended to maintain their FM character when increasing the temperature in both samples.

The presented experimental results of the temperature and field dependence of magnetization, Figs. 5 and 6, suggest that due to the SFM character of the magnetic nanoparticles, in combination with their small size, they could be suitable candidates for various electrotechnical applications due to the non-zero coercivity at room temperature.

As was mentioned above, an irregular hysteresis loop was observed in the pristine Fe sample (Fig. 6). Such irregular hysteresis loops have been observed previously by Vasquez *et al.*,[37] who explained this non-linearity by the variation of the squareness ratio $Q = M_R/M_S$ (defined as the ratio between the remanent and saturation magnetizations) and the coercivity H_C. Therefore, we have determined the coercivity H_C, remanent magnetization M_R and saturation magnetization M_S at various temperatures for both Fe and Fe@SiO_2 samples, see Fig. 7.

The theoretical values for the squareness ratios for particles with uniaxial magnetocrystalline anisotropy and for particles with cubic magnetocrystalline anisotropy are $Q = 0.5$ and $Q = 0.831$, respectively.[38] Our low obtained values of squareness ratio (below $Q = 0.5$) show that individual particles are created as single domains,[39] nevertheless the sample without SiO_2 shell (squareness ratio of $Q = 0.16$ at 2 K) exhibits the higher contribution of random magnetic anisotropy than sample with silica shell (squareness ratio

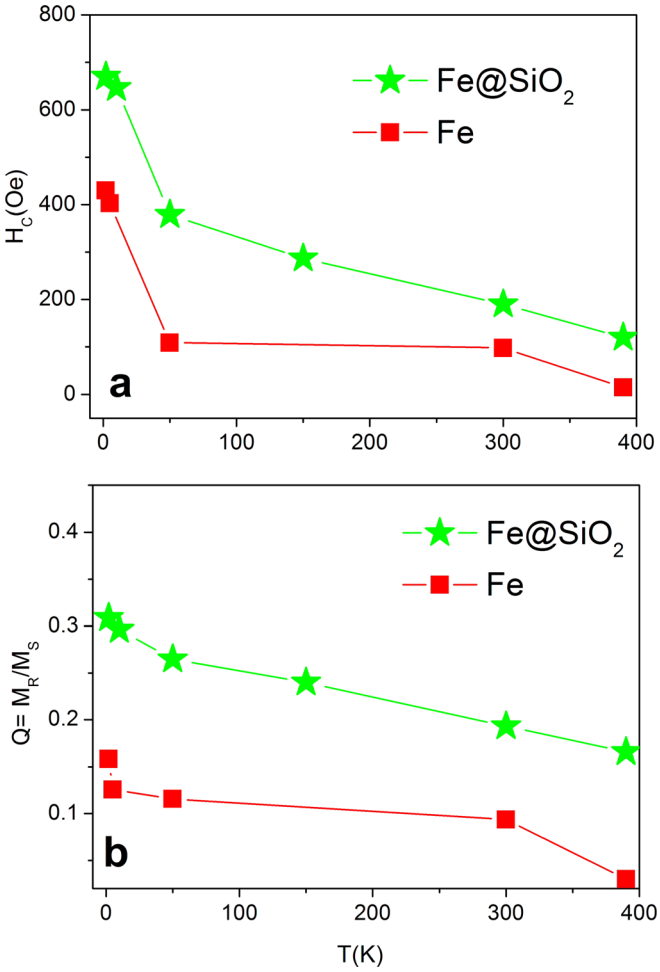

FIG. 7. Comparison of the temperature dependence of the coercive field H_C and the squareness ratio, $Q = M_R/M_S$, for Fe and Fe@SiO_2 samples.

$Q = 0.32$ at 2 K). Also, low values indicate that there are strong interparticle interactions which in the case of the pristine Fe nanoparticles are giving rise to "constricted loops," due to the different assembly of the nanoparticles when they are coated and when they are uncoated.

Moreover, irregular hysteresis loop and the squareness ratio show an additional exchange interaction, which can be associated with the existence of an exchange bias effect.[38,40] We have measured the hysteresis loops at 2 K after cooling in zero field (ZFC loop) and after cooling in external field of 30 000 Oe (FC) in both samples (Fe and Fe@SiO2). In both samples was observed the negative exchange bias effect. The value of exchange bias field H_{EB} calculated from experimental FC hysteresis loops were $H_{EB} = 52$ Oe in the sample Fe@SiO2 and $H_{EB} = 48$ Oe in the Fe sample. These values are comparable; therefore, the intra-particle exchange interaction induced from different magnetic ordering between surface and volume of the particles is almost the same in both samples. Comparable value of exchange bias field confirms that despite of the oxidation of Fe particles in pristine Fe sample, this has no influence on the creation of additional intra-particle exchange interaction.

The differences in magnetic properties between the pristine Fe sample and the Fe@SiO_2 sample can be attributed to

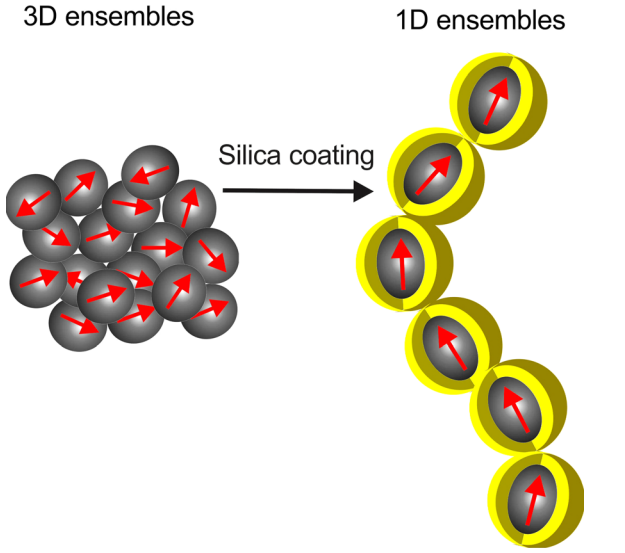

FIG. 8. Schematic of the sample morphology: 3D randomly organized magnetic moments in pristine Fe nanoparticles and 1D chain-like structure in silica coated nanoparticles.

the different spatial organization of nanoparticles. A similar trend was observed by Salgueirino-Maceira *et al.*,[21] who reported that the strong dipolar magnetic interactions present in 1D chains of silica-coated cobalt nanoparticles lead to direct exchange interactions, and to the ferromagnetic state. Based on the presented investigation, we suggest the concept of the particle ordering illustrated in Fig. 8. In pristine Fe NPs, consisting of 3D agglomerates, the magnetic moments of particles are oriented randomly, which led to the smaller value of magnetic anisotropy. In contrast, the mono-domain particles coated by a silica shell (Fe@SiO_2) are organized into 1D chains. Such spatial organization promotes the higher magnetic anisotropy of the ensembles.

IV. CONCLUSION

We have prepared Fe nanoparticles coated with an SiO_2 layer, which promotes the self-organization of nanoparticles into 1D chain-like structures. Transmission electron microscopy indicated the average size of prepared nanoparticles was about $D_{avg} \sim 4$ nm for pristine Fe NPs and $D_{avg} \sim 13$ nm for the Fe@SiO_2 sample (including silica coating). The XANES spectra show that the coating of nanoparticles by the silica layer prevents the further surface oxidation of the iron cores. Magnetization studies show that the prepared nanoparticles exhibit strong dipolar magnetic interactions leading to the long-range ordering (exchange interactions) of magnetic moments, and the system exhibits SFM properties. The observed SFM behavior renders the studied material a good candidate for applications in microelectronics as a high-permeability, low-loss material and in sensing devices designed for high frequencies.

ACKNOWLEDGMENTS

This work was supported by the Slovak Research and Development Agency under the contract APVV-0222-10 and APVV-0132-11 and VEGA (Nos. 1/0583/11 and 1/0861/12)

projects of Ministry of Education of the Slovak Republic and by the ERDF EU grant under No. ITMS 26220220105. The authors (A.Z. and V.Z.) would like to thank DESY/HASYLAB project under No. I-20110282 EC. The authors would like to thank Dr. Paula Lampen for help with revisions of the manuscript.

[1]S. A. Majetich, *Nanostructured Materials: Processing, Properties, and Applications*, 2nd ed. (William Andrew Inc., USA, 2007), pp. 439–486.
[2]C. L. Dennis, R. P. Borges, L. D. Buda, U. Ebels, J. F. Gregg, M. Hehn, E. Jouguelet, K. Ounadjela, I. Petej, I. L. Prejbeanu, and M. J. Thornton, J. Phys.: Condens. Matter. **14**, R1175–R1262 (2002).
[3]C. Djurberg, P. Svedlindh, P. Nordblad, M. F. Hansen, F. Bødker, and S. Mørup, Phys. Rev. Lett. **79**, 5154–5157 (1997).
[4]J. M. Vargas, W. C. Nunes, L. M. Socolovsky, M. Knobel, and D. Zanchet, Phys. Rev. B **72**, 184428 (2005).
[5]S. Karmakar, S. Kumar, R. Rinaldi, and G. Maruccio, J. Phys.: Conf. Ser. **292**, 012002 (2011).
[6]A. K. Gupta and M. Gupta, Biomaterials **26**, 3995–4021 (2005).
[7]Q. A. Pankhurst, J. Connolly, S. K. Jones, and J. Dobson, J. Phys. D: Appl. Phys. **36**, R167 (2003).
[8]T. Jonsson, P. Nordblad, and P. Svedlindh, Phys. Rev. B **57**, 497 (1998).
[9]O. Petracic, X. Chen, S. Bedanta, W. Kleemann, S. Sahoo, S. Cardoso, and P. P. Freitas, J. Magn. Magn. Mater. **300**, 192 (2006).
[10]S. Mørup, M. F. Hansen, and C. Frandsen, Beilstein J. Nanotechnol. **1**, 182–190 (2010).
[11]V. Markovich, I. Fita, A. Wisniewski, G. Jung, D. Mogilyansky, R. Puzniak, L. Titelman, and G. Gorodetsky, Phys. Rev. B **81**, 134440 (2010).
[12]M. Suzuki, S. I. Fullem, I. S. Suzuki, L. Wang, and C. J. Zhong, Phys. Rev. B **79**, 024418 (2009).
[13]S. Sahoo, O. Petracic, Ch. Binek, W. Kleemann, J. B. Sousa, S. Cardoso, and P. P. Freitas, Phys. Rev. B **65**, 134406 (2002).
[14]S. Morup, M. B. Madsen, J. Franck, J. Villadsen, and C. J. W. Koch, J. Magn. Magn. Mater. **40**, 163 (1983).
[15]W. Kleemann, O. Petracic, Ch. Binek, G. N. Kakazei, Y. G. Pogorelov, J. B. Sousa, S. Cardoso, and P. P. Freitas, Phys. Rev. B. **63**, 134423 (2001).
[16]S. Bedanta, T. Eimüller, W. Kleemann, J. Rhensius, F. Stromberg, E. Amaladass, S. Cardoso, and P. P. Freitas, Phys. Rev. Lett. **98**, 176601 (2007).
[17]S. Bedanta and W. Kleemann, J. Phys. D: Appl. Phys. **42**, 013001 (2009).
[18]J. Alonso, M. L. Fdez-Gubieda, J. M. Barandiarán, and A. Svalov, Phys. Rev. B **82**, 054406 (2010).
[19]F. Jimenez-Villacorta, J. Sanchez-Marcos, E. Cespedes, M. García-Hernández, and C. Prieto, Phys. Rev. B **82**, 134413 (2010).
[20]T. I. Yang, R. N. C. Brown, L. C. Kempel, and P. Kofinas, Nanotechnology **22**, 105601 (2011).
[21]V. Salgueirino-Maceira, M. A. Correa-Duarte, A. Hucht, and M. Farle, J. Magn. Magn. Mater. **303**, 163–166 (2006).
[22]M. Grzelczak, J. Perez-Juste, B. Rodriguez-Gonzalez, M. Spasova, I. Barsukov, M. Farle, and L. M. Liz-Marzan, Chem. Mater. **20**, 5399 (2008).
[23]Y. Kobayashi, M. Horie, M. Konno, B. Rodriguez-Gonzalez, and L. M. Liz-Marzan, J. Phys. Chem. B **107**, 7420 (2003).
[24]A. P. Hammersley, S. O. Svensson, M. Hanfland, A. N. Fitch, and D. Häusetmann, High Press. Res. **14**, 235 (1996).
[25]S. Kraft, J. Stumpel, P. Becker, and U. Kuetgens, Rev. Sci. Instrum. **67**, 681–687 (1996).
[26]Y. P. Sun, X. Li, J. Cao, W. Zhang, and H. P. Wang, Adv. Colloid Interface Sci. **120**, 47–56 (2006).
[27]G. Cheng, J. D. Carter, and T. Guo, Chem. Phys. Lett. **400**, 122–127 (2004).
[28]J. B. Sousa, J. A. M. Santos, R. F. A. Silva, J. M. Teixeira, J. Ventura, J. P. Araújo, P. P. Freitas, S. Cardoso, Y. G. Pogorelov, G. N. Kakazei, and E. Snoeck, J. Appl. Phys. **96**, 3861 (2004).
[29]M. F. Hansen, C. B. Koch, and S. Mørup, Phys. Rev. B **62**, 1124 (2000).
[30]F. Mazaleyrat, J. C. Faugières, and J. F. Rialland, J. Magn. Magn. Mater. **159**, L33–L38 (1996).
[31]A. Zelenakova, J. Kovac, and V. Zelenak, J. Appl. Phys. **108**, 034323 (2010).
[32]M. Tadic, V. Kusigerski, D. Markovic, I. Milosevic, and V. Spasojevic, J. Magn. Magn. Mater. **321**, 12–16 (2009).
[33]G. Herzer, *Handbook of Magnetic Materials* (Elsevier Science, 1997), vol. **10**, pp. 415–462.
[34]G. Herzer, IEEE Trans. Magn. **26**, 1397–1402 (1990).
[35]M. Solzi, C. H. Pernechele, G. Calestani, M. Villani, M. Gaboardi, and A. Migliori, J. Mater. Chem. **21**, 18331–18338 (2011).
[36]D. C. Lee, F. V. Mikulec, J. M. Pelaez, B. Koo, and B. A. Korgel, J. Phys. Chem. B **110**, 11160–11166 (2006).
[37]C. Vasquez-Vasquez, M. A. Lopez-Quintela, M. C. Bujan-Nunez, and J. Rivas, J. Nanopart. Res. **13**, 1663–1676 (2011).
[38]J. Garcia-Otero, M. Porto, J. Rivas, and A. Bunde, J. Appl. Phys. **85**, 2287 (1999).
[39]N. E. Fenineche, R. Hamzaoui, and O. El Kedim, Mater. Lett. **57**, 4165–4169 (2003).
[40]A. Zelenakova, J. Kovac, and V. Zelenak, Acta Phys. Pol. A **115**, 357–359 (2009); available at http://przyrbwn.icm.edu.pl/APP/PDF/115/a115z1103.pdf.